ACS Catalysis

Research Article

pubs.acs.org/acscatalysis

Methane Activation in Gold Cation-Exchanged Zeolites: A DFT Study

Sippakorn Wannakao,[†,‡,§,∥] Chompunuch Warakulwit,[†,‡,§,∥] Kanokwan Kongpatpanich,[†,‡,§,∥] Michael Probst,[⊥] and Jumras Limtrakul*[,†,‡,§,∥]

[†]National Center of Excellence for Petroleum, Petrochemicals and Advanced Materials, Department of Chemistry, Faculty of Science, Kasetsart University, Bangkok 10900, Thailand

[‡]Center for Advanced Studies in Nanotechnology and Its Applications in Chemical, Food and Agricultural Industries, Kasetsart University, Bangkok 10900, Thailand

[§]NANOTEC Center of Excellence, National Nanotechnology Center, Kasetsart University, Bangkok 10900, Thailand

[∥]Center of Nanotechnology, Kasetsart University Research Development Institute, Kasetsart University, Bangkok 10900, Thailand

[⊥]Institute of Ion Physics and Applied Physics, University of Innsbruck, 6020 Innsbruck, Austria

Supporting Information

ABSTRACT: Activation of methane has attracted a great deal of interest in laboratory chemical synthesis and in large-scale industrial processes. We performed density functional theory studies to investigate the C−H bond breaking of methane on Au^+ and Au_2^+ ions in vacuum and inside different types of zeolites. The density functional M06-L and the 6-31G(d,p) basis set were employed as this level of theory had already been shown to be reasonably accurate and affordable for transition metal systems. We investigated four industrially important catalysts, ZSM-5, FAU, FER, and MCM-22, each with a particular framework topology, with respect to their performance for methane activation. The bicoordinated character of the cationic site in the ZSM-5 structure provides a higher activity than the FAU structure with a 3-fold coordination of its cationic site. The activation energy of the reaction catalyzed by Au-ZSM-5 is lower than the one with the bare Au^+ cation (13.2 vs 21.3 kcal/mol) because of the structural constraint imposed by the zeolite that leads to an earlier transition state with a high charge difference of the C−H atoms where the bond is broken. It is also found that the activity of Au_n^+ decreases already with $n = 2$, due to the shared positive charge. For the zeolites with large pores, Au-MCM-22 provides a higher activity due to the spacious framework of this particular type of zeolite is perfect for stabilizing the transition state structure but not the corresponding adsorption complex. The small and medium pore-sized zeolites, Au-FER and Au-ZSM-5 stabilize both the adsorption complex and the transition states, thus causing the activation energy to remain the same.

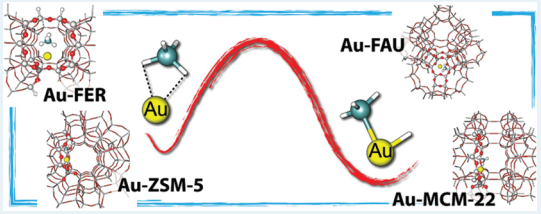

KEYWORDS: *methane activation, gold, catalyst, density functional theory, transition state*

INTRODUCTION

The chemical transformation and functionalization of light hydrocarbons has been called "the holy grail of chemistry".[1] Such hydrocarbons are the main constituents of oil and natural gas, a feedstock for the chemical industry that transforms them to more valuable products. Typically, the cleavage of a C−H bond is the important initial step of these chemical transformations. Because of the stability of this bond, this is surprisingly difficult.[2] Among the light alkanes that have been investigated for C−H activation, methane is attracting a great deal of interest due to the fact that it can be obtained in large quantities from petrologic natural gas and that it is also a renewable biochemical resource. Methane can be converted into other valuable products such as methanol, formaldehyde, acetic acid or light olefins, and ethylene.[3−9] The cleavage of the C−H bond of methane requires a high energy of about ∼100 kcal/mol[10] and its activation by means of catalysts is still a subject of fundamental research.[9] Metals in the form of ions,[11,12] complexes, surfaces,[13] clusters,[14] cluster ions,[15−17] oxides,[18,19] metal-exchanged zeolites,[20−23] and many more have been considered as catalysts. Fundamental information comes often from gas phase metal clusters or metal ions, typically produced in sophisticated mass-spectroscopic experiments. For production, heterogeneous catalysts are used on an industrial scale. Metal-exchanged zeolites hold promise in this aspect because they possess the characteristics of heterogeneous catalysts, like an easy separation of the catalyst from the reaction mixture at the end of the reaction. Their catalytic activity is connected to the nature of the zeolite frameworks.

A considerable number of theoretical[20,21,23] and experimental[22,24,25] studies have investigated the C−H activation of methane catalyzed by metal-exchanged zeolites. All of these studies investigated Fe-, Mo-, Ag-, or Cu-exchanged ZSM-5. To the best of our knowledge, the methane activation catalyzed by Au-exchanged zeolites has not yet been examined and this is the scope of our present work. The successful synthesis of MFI

Received: December 12, 2011
Revised: February 24, 2012
Published: April 18, 2012

   dx.doi.org/10.1021/cs200653q | ACS Catal. 2012, 2, 986−992

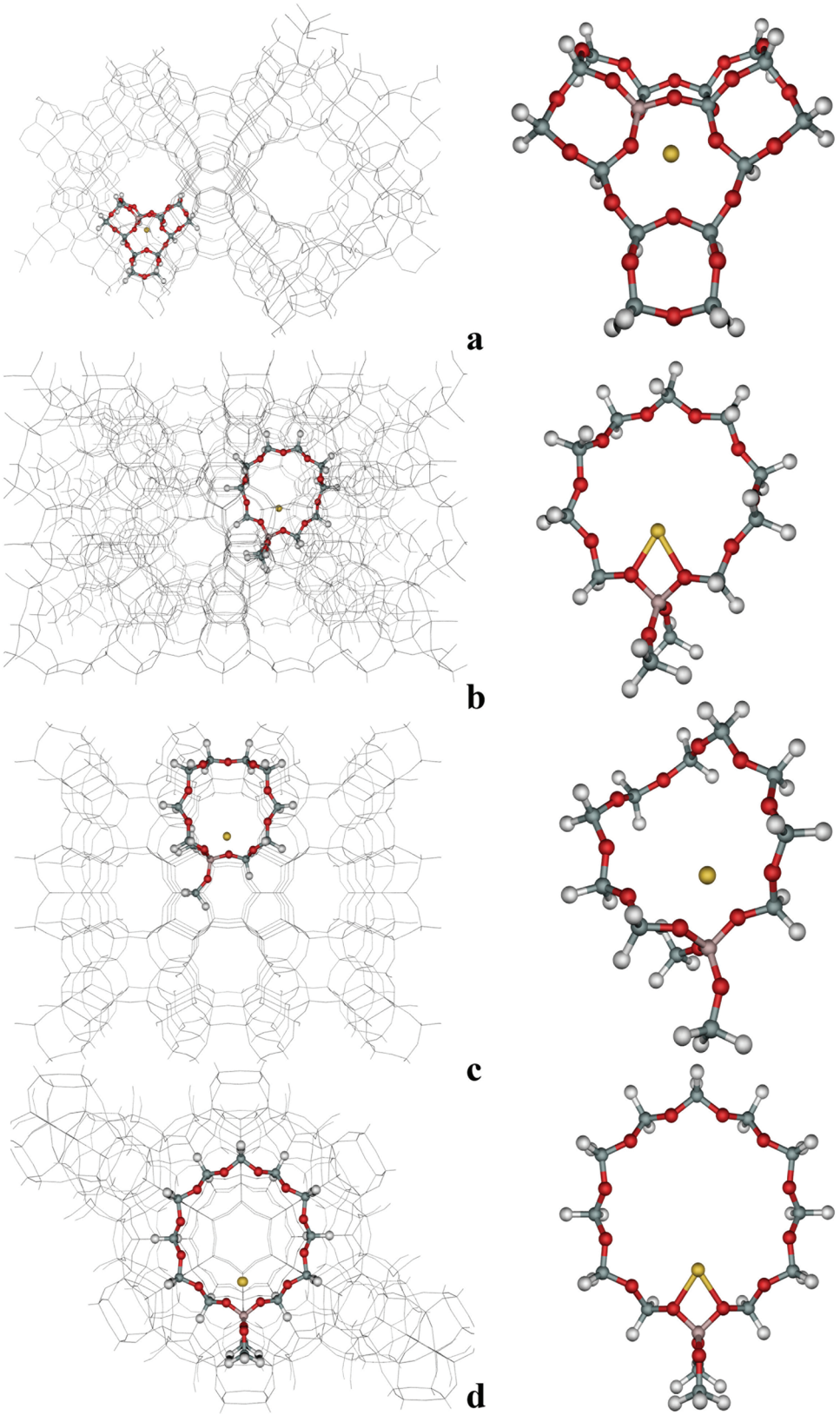

Figure 1. Cluster models of (a) Au-FAU, (b) Au-ZSM-5, (c) Au-FER, and (d) Au-MCM-22.

and NaY type Au-exchanged zeolites, including Au-NaY, Au-NaZSM-5, Au-ZSM-5, and less frequently, Au-NaMOR,[26−32] has already been reported. Recently, Ichikawa et al.[26,31] used CO adsorption to study Au/NaY, Au/Na-MOR, and Au/Na-ZSM-5 and concluded that Au^+ is the dominant active site on which the reactions take place.

Conversely, also methane activation by dimeric gold cations (Au_2^+)[17,33] was recently reported. Despite the likely presence of gold ions (Au_x^{n+}) with even more different oxidation states and

dx.doi.org/10.1021/cs200653q | ACS Catal. 2012, 2, 986−992

charged as well as neutral gold (Au_x) clusters inside the structures and on the external surface of the zeolites, only Au^+ and Au_2^+ were considered by us as active species.

In this work, we study the activation of the methane C−H bond on Au-exchanged zeolites, namely faujasite (FAU), ZSM-5, ferrierite (FER) and MCM-22 with the M06-L density functional. We investigate those factors that are expected to be relevant for the reactivity, for example the cationic coordination site, the size of the pore channel and the effect of framework structures. First, we compare coordination sites on FAU and ZSM-5 with each other and then the effect of the pore channel size in FER, ZSM-5, and MCM-22. For this, small cluster models are used while the effect of different frameworks on the stabilities of adsorption and transition states is studied with larger clusters, without considering geometric relaxation. Since the C−H bond of methane is especially strong, the results of this study could be relevant for developing catalysts for the activation of other hydrocarbons.

METHODOLOGY

The zeolite cluster models were taken from the crystallographic data of H-ZSM-5, H-FAU, H-FER, and H-MCM-22 zeolites.[34−36] Small clusters with a local cationic site were selected for calculation. They are shown in Figure 1. For the case of Au(I)-exchanged ZSM-5 (Au-ZSM-5), a 12T cluster model was used. This model covers the 12-membered-ring window (5.1 × 5.4 Å) representing the intersection cavity where the straight channel and the zigzag channel cross. The molecules cross this intersection cavity with the highest probability. The question of the preferred position of the aluminum atom in ZSM-5 zeolite was widely studied experimentally[37−39] and theoretically.[37,40,41] The exact position cannot be determined because the energies of the aluminum replacement at different T sites differ very little from each other and calculation of NMR shifts[37] to which experimental spectra could be compared is not yet quite as accurate as would be required. Most studies indicate that at least part of the aluminum sits on the T12 site.[38,40] In our model, a silicon atom was substituted by an aluminum atom at the T12 position in the same way as has been done in former theoretical studies.[42−44] For the case of Au(I)-exchanged FAU (Au-FAU), the 16T cluster that represents the supercage of FAU was selected. Even in the case of FAU, there are several possible sites where the cation can reside. We choose site II, the 6-membered ring of the T atoms which is confirmed by various experimental studies as the site with the highest cation occupation.[45,46] For Au(I)-exchanged FER (Au-FER), a 10T cluster model was used. This model covers the 10-membered ring window (4.2 × 5.4 Å) where the main channel and the 8-membered ring channel intersect. There, a silicon atom at the T2 site was replaced by an aluminum atom to represent the Brønsted acid site.[47] Finally, for Au(I)-exchanged MCM-22 (Au-MCM-22), a 12T cluster model representing the 12-membered ring channels of the supercage (7.1 × 7.1 × 18.4 Å) was selected. The substituted aluminum atom is located at the T1 site to model the Brønsted acid site.[48] In all cases, the Au^+ ion was located to bridge two oxygen atoms at their Brønsted acid site. The O atoms at the edge of the cluster were fixed in their crystallographic positions. H atoms were used to terminate the O atoms at the edge of the model along the direction of the crystallographic O−Si bonds with the O−H bond length of 1.47 Å. Only a portion of 5T around the Al atom of Au-ZSM-5, Au-FER and Au-MCM-22 and 4T at the 6-membered ring of Au-FAU and the probe molecule were allowed to relax during geometry optimizations, as in our previous studies.[49−52]

The M06-L density functional[53−55] takes dispersion into account by means of its parametrization and has been shown to be both accurate for transition metals and affordable for large systems like the ones studied here.[49−52,56−60] Madsen et al.[56,61] recently showed that this functional performs also quite well for the 2D-3D transition of ionic gold clusters and for the covalent and dispersive interaction in layered solids. We used M06-L together with the Stuttgart effective core potential[62] and its basis set for Au and the 6-31G(d,p) basis set for all other atoms. Addition of diffuse functions does not influence the energetics. Test calculations on Au-ZSM-5 and Au-FER with the 6-31+G(d,p) basis set are shown in the Supporting Information. Transition state structures were checked by normal-mode analysis. In all cases we found only one imaginary frequency, corresponding to the reaction coordinate, and even the frequencies of the modes involving terminating atoms are all real. According to the work of Li and Armentrout,[12] a low spin multiplicity of the Au atom is favorable, and all systems containing Au^+ were considered to be in the singlet state, the electronic ground state of Au^+. Systems with Au_2^+ were assumed to be in the doublet state. To observe the influence of the framework structures to energies during the reaction on different zeolites we additionally performed single-point calculations on each zeolitic framework with large 120T clusters using the same level of theory. Natural bond orbital (NBO)[63,64] analysis was used to describe the partial charges of all systems. All calculations were performed with the Gaussian 03 package,[65] modified to incorporate the Minnesota density functionals module 3.1 by Zhao and Truhlar.

RESULTS AND DISCUSSION

1. Methane Activation on Bare Au^+ and Au_2^+ Ions. First, our methodology was applied on the C−H bond breaking of methane in the gas phase ionic systems with bare Au^+ and Au_2^+ ions in their electronic ground in which are singlet and doublet states, respectively. The calculated Au−Au distance in Au_2^+ is 2.69 Å and its dissociation energy amounts to 45.1 kcal/mol. This underestimates experimental values by about ∼5 kcal/mol.[66] Distance and dissociation energy values are very close to high-level of theory CCSD(T)[67] results.

The calculated adsorption energies (E_{ads}), activation energies (E_a), and reaction energies (E_r) of the methane/Au^+ and Au^{2+} systems are shown in Table 1. Optimized structures of the adsorption state, transition state and the dissociated products are given in Figure 2. Methane adsorbs more strongly to Au^+ (−20.7 kcal/mol) than to Au_2^+ (−16.6 kcal/mol). This is consistent with the shorter Au−C distance for Au^+ (2.44 Å) vs Au_2^+ (2.53 Å). The NBO charge of the Au atom in Au-CH_4^+ is +0.90|e| and the charge of the C atom is −1.050|e|. In the case of the Au_2^+ system, the two Au atoms carry NBO charges of +0.42|e| and +0.49|e| for Au and −1.01|e| for C. The C and H atomic charges of the isolated methane molecule are −0.96|e| and +0.24|e|, respectively. Thus, it is found that the Au^+ induces a negative charge on the C atom.

As expected from the discussion above, Au^+ lowers the activation barriers E_a of the C−H activation more than Au_2^+. The barrier heights are 21.3 and 29.7 kcal/mol. In all respects, the relatively small Au^+ cation with its high charge density provides stronger methane adsorption and better activation than Au_2^+ where the single charge is spread out over two atoms

dx.doi.org/10.1021/cs200653q | ACS Catal. 2012, 2, 986−992

Table 1. Adsorption Energy (E_{ads}), Activation Energy (E_a) and Reaction Energy (E_r) of the C−H Activation of Methane over the Au-ZSM-5 and the Au-FAU Systems (kcal/mol)[a]

systems	E_{ads}	E_a	E_r
Au^+	−20.7	21.3	−0.9
Au_2^+	−16.6	29.7	−16.6
Au-ZSM-5 (Pathway A)	−18.9	13.2	−10.1
Au-ZSM-5 (Pathway B)		32.0	−18.8
Au_2-ZSM-5 (Pathway A)	−8.1	22.2	8.7
Au_2-ZSM-5 (Pathway B)		33.2	4.3
Au-FAU (Pathway A)	−11.1	22.2	5.1
Au-FAU (Pathway B)		31.7	4.4
Au_2−FAU (Pathway A)	−6.0	27.2	13.3
Au_2−FAU (Pathway B)		30.8	13.5

[a] E_r is the energy difference between the dissociative product and the reactants ($E_{dissociative\ product} - E_{reactants}$).

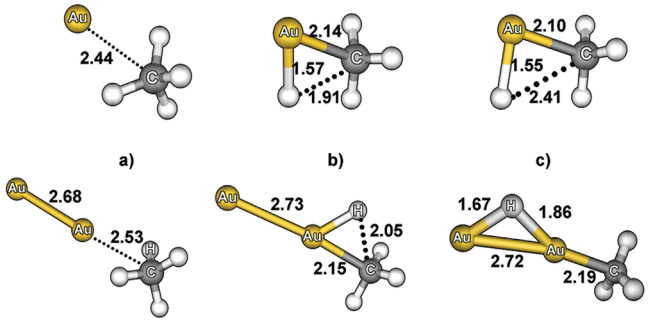

Figure 2. Optimized structures (M06-L/6-31G(d,p) calculations) of (a) adsorption state, (b) transition state, and (c) dissociative product with some interatomic distances (Å) for the methane activation over the Au+ (upper graphs) and Au_2^+(lower graphs) ions.

and the Au−Au bond. The dissociation intermediates of the Au^+ and Au_2^+ systems differ in structure and stability. The dissociating H atom is located in a bridge position between the two Au atoms of the Au_2^+ system (see Figure 2c). This intermediate is stabilized by −16.6 kcal/mol while for Au^+, the intermediate is only 0.9 kcal/mol more stable than the reactants. These results mean that in the C−H activation, the Au_2^+ intermediate is thermodynamically preferred while the Au^+ intermediate is more kinetically favored. We did not investigate larger gold clusters in which the reactivity is normally increasing with the number of unsaturated gold surface atoms and the charge. Other parameters such as shape and size also influence their electronic structure, so that their catalytic behavior cannot be predicted easily.[68,69]

2. Methane Activation over Au^+ and Au_2^+ Cation-Exchanged Zeolites. To understand the effects of the local cation sites in zeolites, we first study the FAU and ZSM-5 systems with their different active site structures. The NBO charge of Au in the Au-ZSM-5 cluster is +0.75|e|. In Au-FAU the Au charge has a lower value of +0.70|e|, because of the three surrounding oxygen atoms, compared to two in Au-ZSM-5. The lower charge goes along with a lower adsorption energy of methane over the Au-FAU (E_{ads} = −11.1 kcal/mol) compared to those of the Au-ZSM-5 (E_{ads} = −18.9 kcal/mol). The complexation of the Au^+ cation and the negatively charged zeolite clusters is exothermic by 154.2 and 152.4 kcal/mol for Au-FAU and the Au-ZSM-5, respectively. The introduction of the second gold atom to Au-ZSM-5 and Au-FAU is exothermic by about 35 kcal/mol in both cases but this value is smaller than the dissociation energy of the Au−Au bond (~45 kcal/mol) in the free Au_2^+ ion.

The difference in the active site characteristics of the zeolites does not much affect the adsorption energies in the Au_2^+ systems: The energies of adsorption of methane in the Au_2^+ ion in Au_2-ZSM-5 and in Au_2−FAU are −16.6, −8.1, and −6.0 kcal/mol, respectively. The Au atom where the methane C atom becomes adsorbed (the "Au_{ac}" atom) is already deactivated and the additional influence of the zeolite framework is small. Its NBO charges in Au_2-ZSM-5 and Au_2−FAU are +0.33|e| and +0.25|e|, respectively. The presence of the zeolite frameworks decreases the adsorption energy. Two pathways for methane activation over the Au-zeolites are possible. In the first one, methane dissociates over the Au^+ ion. Then the CH_3 group and the H atom stay coordinated to the Au^+ ion (Pathway A). In the other pathway, methane dissociates over both the Au^+ ion and an O atom of the zeolite framework. One H atom of methane migrates to the O atom while CH_3 still binds to the Au atom (Pathway B). The reaction mechanisms of Pathways A and B are summarized in Scheme 1.

Scheme 1. Reaction Scheme of Pathways A and B

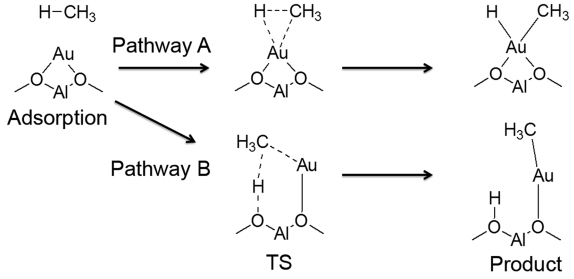

Both pathways lead to charge polarization between the CH_3 group and the H atom, respectively ($CH_3^{\delta-}$−$H^{\delta+}$). They can be considered to be different pathways of the same "alkyl" activation which was proven to be favorable for methane activation over Ag-ZSM-5 by the group of Huang.[21] The reaction energies for both pathways are shown in Table 1.

Our results indicate a preference of Pathway A for both the reactions over Au-ZSM-5 and Au_2-ZSM-5. The presence of ZSM-5 zeolite reduces the activation energies from 21.3 and 29.7 kcal/mol for the bare Au^+ and Au_2^+ systems to 13.2 and 22.2 kcal/mol, respectively.

In the FAU systems with Au^+ and Au_2^+ as active species, the activation energy of Pathway A is again the lower one and it should be the preferred one for both Au^+ and Au_2^+. Here the presence of the FAU framework does not decrease the activation barriers which are similar to the bare ion cases, unlike ZSM-5 (Table 1).

To understand the activity of Au-ZSM-5 over the gold cations, we analyzed structural parameters and atomic populations. The Au partial charge in Au-ZSM-5 is 0.75|e|, 0.58|e| and 0.71|e| at the bare-catalyst, methane adsorption and transition state, respectively. The corresponding values for pure Au^+ are 1.00|e|, 0.90|e|, and 0.73|e|, respectively. Even though the Au charges at the transition state are similar, Au-ZSM-5 induces a much smaller positive partial charge into methane than the Au^+ cation (0.01|e| vs 0.27|e|). The charge differences between the C and H atoms involved in the bond breaking process are 1.03|e| and 0.89|e| for the Au-ZSM-5 and Au^+ cation, respectively with C−H bond distances at the transition states of 1.67 and 1.91 Å, respectively. Again this is correlated

dx.doi.org/10.1021/cs200653q | ACS Catal. 2012, 2, 986−992

to the C−H distances in the intermediates which are 2.31 and 2.42 Å for the Au-ZSM-5 and Au^+ system, respectively. The shorter C−H distances in the zeolite system imply that the constraints imposed by the ZSM-5 structure play a role in its higher activity as well as in stabilizing the product over the Au^+ cation (see Figures 2 and 3). This structural constraint leads to an earlier transition state of Au-ZSM-5.

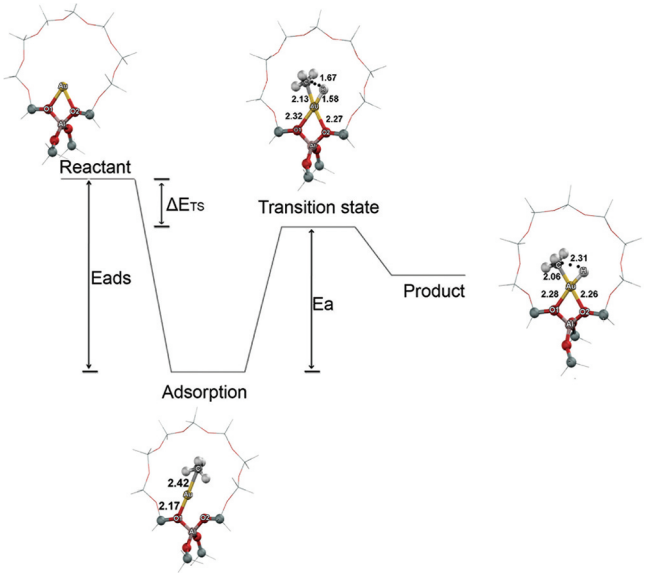

Figure 3. Reaction profile of Pathway A on Au-ZSM-5 and reference energies that are used in this work, namely, adsorption energy (E_{ads}), activation energy (E_a), and transition state energy (ΔE_{TS}).

For Au-FAU, we found a C−H distance of 1.75 Å and a charge difference of 0.89|e| at the transition state. These values are close to the ones of the Au^+ ion system. The FAU framework cannot increase the activity of Au^+ at its local site.

From this part it can be summarized that the activation energy is lower than the adsorption energy only in Au-ZSM-5 while for the rest of the systems the adsorption energy is lower (see Table 1). This, of course, would indicate that in Au-ZSM-5 C−H bond breaking rather than only methane adsorption occurs. This issue was also studied for the cationic sites in the zeolite channels of FER and MCM-22 which have smaller and larger pore structures, respectively, than ZSM-5.

3. Methane Activation over Au-FER and Au-MCM-22 Compared to Au-ZSM-5. In the same way as described above, we investigated the reaction over FER and the MCM-22 zeolites. FER has a smaller pore size than that of the ZSM-5, while MCM-22 has a larger one. These zeolites were studied with a bicoordinated Au atom to keep the character of the active site the same. Thus, only effects of frameworks are elucidated. For simplicity, we investigated only the Au^+ systems and Pathway A since they can be assumed to be the most important also for these systems as they were for ZSM-5 and FAU as discussed above.

Both Au-FER and Au-MCM-22 provide lower adsorption energies compared to Au-ZSM-5. The adsorption energies are −16.8 and −16.5 kcal/mol for Au-MCM-22 and Au-FER, respectively. The activation barrier in the larger pore structure of MCM-22 is lower than in Au-FER. The values of E_a of the methane activation over Au-FER and Au-MCM-22 are 15.0 and 12.0 kcal/mol, respectively. Like in Au-ZSM-5, the polarization of the breaking C−H bond expressed as partial charge differences, is in the same order as the E_a values (Au-MCM-22 ≈ Au-ZSM-5 > Au-FER > bare Au^+) and as the C−H distances which have values of 1.63, 1.67, and 1.70 Å for Au-MCM-22, Au-ZSM-5, and Au-FER, respectively. The charge differences and bond distances are summarized in Table 2.

Table 2. Geometrical Parameters of the Transition States (TS) and Adsorption Energies for Au^+ and for the Small and Large Zeolite Models

parameters	Au^+	Au-ZSM-5	Au-FER	Au-MCM-22
TS C−H distance	1.91	1.67	1.70	1.63
TS C−H charge difference	0.89	1.03	1.00	1.02
		adsorption energy		
molecular model	−20.7	−18.9	−16.5	−16.8
nano model		−21.0	−18.3	−16.7
		ΔE_{TS}[a]		
molecular model	0.6	−5.7	−1.5	−4.8
nano model		−8.2	−4.3	−7.0
		activation energy		
molecular model	21.3	13.2	15.0	12.0
nano model		12.8	14.1	9.7

[a] ΔE_{TS} is the relative energy of the transition state compared to the isolated reactants ($\Delta E_{TS} = E_{TS} - E_{reactant1} - E_{reactant2} - \ldots$).

The above investigations were extended by single point calculations on the 120T framework structure for Au-ZSM-5, Au-MCM-22 and Au-FER in order to evaluate the effect of long-range interactions that the small models cannot cover. The structure of those zeolite pores is shown in Figure 4. Additionally, geometry optimization of Au-ZSM-5 and Au-FER were performed on larger 46T clusters which cover the pore structures. They show the same energetic trend as in the relaxed 12T clusters (see Table S1 in Supporting Information). From here on, we only discuss the 120T single point results. For Au-ZSM-5 and Au-FER, this results in slightly higher adsorption energies of −21.0 and −18.3 kcal/mol, respectively. The activation energies change even less (12.7 and 14.0 kcal/mol, respectively). For the structure with larger pores, Au-MCM-22, the adsorption energy does not change but the transition state is more stabilized, resulting in an activation energy of 9.7 kcal/mol. Altogether, in the extended Au-MCM-22, Au-ZSM-5, and Au-FER clusters the energy of transition structures (ΔE_{TS}) decrease by 2.1, 2.5, and 2.9 kcal/mol, respectively, compared to the small clusters. For Au-MCM-22 this can be explained by long-range interactions which do not play a role for the adsorption of CH_4 but do so for the ion-pair like transition state, thereby reversing the trend between the activation energies and the pore size found in Au-MCM-22 and Au-FER. A smaller activity in small pores has also been observed before for the acetone keto−enol tautomerization on H-ZSM-5, H-FER and H-MCM-22.[70] There, the large cavity of MCM-22 zeolite is best suitable for the bulky enol form of acetone molecule.

CONCLUSION

The activation of the methane C−H bond on Au-cation-exchanged zeolites was investigated by calculations with the M06-L density functional. For the methane activation on Au^+-exchanged zeolites, we found that the cationic site is important for the reaction activity: a smaller coordination number of Au,

dx.doi.org/10.1021/cs200653q | ACS Catal. 2012, 2, 986−992

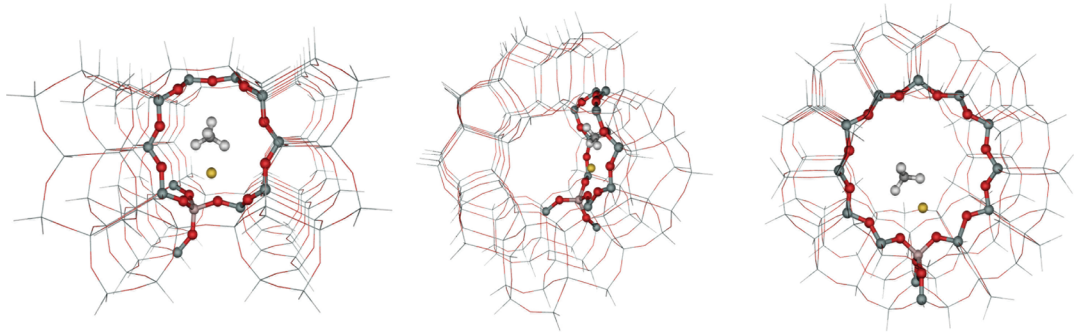

Figure 4. Framework models of Au-FER, Au-ZSM-5, and Au-MCM-22 (left to right, respectively) on which single point calculations were performed, ball and stick parts represent optimized structures.

like in the case of ZSM-5, results in a higher activity than the highly coordinated Au atom in the FAU structure. In the case of ZSM-5, the activation energy of the methane activation is lower than for bare gold cations because of the structural constraints that cause the transition state to appear early in the reaction coordinate. Generally, Au_2^+ is less active than Au^+ because the charge-sharing is not counteracted by a large polarizability. We have studied the effect of pore sizes by comparing Au-FER, Au-ZSM-5 and Au-MCM-22 zeolites which represent structures with small, medium and large pores, respectively. The zeolite with the largest pores, Au-MCM-22 exhibits the highest activity (the lowest activation energy) because of a better stabilization of its transition state structure.

■ ASSOCIATED CONTENT

Ⓢ Supporting Information

As mentioned in text. This material is available free of charge via the Internet at http://pubs.acs.org.

■ AUTHOR INFORMATION

Corresponding Author

*E-mail: jumras.l@ku.ac.th.

Notes

The authors declare no competing financial interest.

■ ACKNOWLEDGMENTS

This work was supported in part by grants from the National Science and Technology Development Agency (NSTDA Chair Professor and NANOTEC Center of Excellence), the Thailand Research Fund (to J.L.), the Kasetsart University Research and Development Institute (KURDI), the Commission on Higher Education, Ministry of Education ("the National Research University Project of Thailand (NRU)" and "Postgraduate Education and Research Programs in Petroleum and Petrochemicals and Advanced Materials"), under the Royal Golden Jubilee Ph.D. program from the Thailand Research Fund (to S.W.). The Graduate School Kasetsart University is also acknowledged. M.P. acknowledges support from the Austrian Research Council (FWF: I200−N19 and RFBR: 09-03-91001-a) and from the Austrian Ministry of Science via an infrastructure grant to the LFU scientific computing platform. The authors are grateful to Donald G. Truhlar and Yan Zhao for supplying them with the code for the M06-L functional.

■ REFERENCES

(1) Schwarz, H. *Angew. Chem., Int. Ed.* **1991**, *30*, 820−821.
(2) Shilov, A. E.; Shul'pin, G. B. *Chem. Rev.* **1997**, *97*, 2879−2932.
(3) Alvarez-Galvan, M. C.; Mota, N.; Ojeda, M.; Rojas, S.; Navarro, R. M.; Fierro, J. L. G. *Catal. Today* **2011**, *171*, 15−23.
(4) Anders, H. *Catal. Today* **2009**, *142*, 2−8.
(5) Arena, F.; Gatti, G.; Martra, G.; Coluccia, S.; Stievano, L.; Spadaro, L.; Famulari, P.; Parmaliana, A. *J. Catal.* **2005**, *231*, 365−380.
(6) Kirillova, M. V.; Kuznetsov, M. L.; Reis, P. M.; da Silva, J. A. L.; da Silva, J.; Pombeiro, A. J. L. *J. Am. Chem. Soc.* **2007**, *129*, 10531−10545.
(7) Parmaliana, A.; Arena, F.; Frusteri, F.; Martinez-Arias, A.; Granados, M. L.; Fierro, J. L. G. *Appl. Catal., A* **2002**, *226*, 163−174.
(8) Periana, R. A.; Mironov, O.; Taube, D.; Bhalla, G.; Jones, C. J. *Science* **2003**, *301*, 814−818.
(9) Schwarz, H. *Angew. Chem., Int. Ed.* **2011**, *50*, 10096−10115.
(10) Blanksby, S. J.; Ellison, G. B. *Acc. Chem. Res.* **2003**, *36*, 255−263.
(11) Irikura, K. K.; Beauchamp, J. L. *J. Phys. Chem.* **1991**, *95*, 8344−8351.
(12) Li, F. X.; Armentrout, P. B. *J. Chem. Phys.* **2006**, 125.
(13) Killelea, D. R.; Campbell, V. L.; Shuman, N. S.; Smith, R. R.; Utz, A. L. *J. Phys. Chem. C* **2009**, *113*, 20618−20622.
(14) Trevor, D. J.; Cox, D. M.; Kaldor, A. *J. Am. Chem. Soc.* **1990**, *112*, 3742−3749.
(15) Koszinowski, K.; Schröder, D.; Schwarz, H. *J. Phys. Chem. A* **2003**, *107*, 4999−5006.
(16) Roithova, J.; Schröder, D. *Chem. Rev.* **2010**, *110*, 1170−1211.
(17) Lang, S. M.; Bernhardt, T. M.; Barnett, R. N.; Landman, U. *Angew. Chem., Int. Ed.* **2010**, *49*, 980−983.
(18) Schröder, D.; Roithová, J. *Angew. Chem., Int. Ed.* **2006**, *45*, 5705−5708.
(19) Feyel, S.; Döbler, J.; Schröder, D.; Sauer, J.; Schwarz, H. *Angew. Chem., Int. Ed.* **2006**, *45*, 4681−4685.
(20) Kurnaz, E.; Fellah, M. F.; Onal, I. *Microporous Mesoporous Mater.* **2011**, *138*, 68−74.
(21) Ding, B.; Huang, S.; Wang, W. *Appl. Surf. Sci.* **2008**, *254*, 4944−4948.
(22) Kim, Y.-H.; Borry Iii, R. W.; Iglesia, E. *Microporous Mesoporous Mater.* **2000**, *35−36*, 495−509.
(23) Yoshizawa, K.; Shiota, Y.; Yumura, T.; Yamabe, T. *J. Phys. Chem. B* **2000**, *104*, 734−740.
(24) Kuroda, Y.; Mori, T.; Sugiyama, H.; Uozumi, Y.; Ikeda, K.; Itadani, A.; Nagao, M. *J. Colloid Interface Sci.* **2009**, *333*, 294−299.
(25) Dubkov, K. A.; Sobolev, V. I.; Talsi, E. P.; Rodkin, M. A.; Watkins, N. H.; Shteinman, A. A.; Panov, G. I. *J. Mol. Catal. A: Chem.* **1997**, *123*, 155−161.
(26) Qiu, S.; Ohnishi, R.; Ichikawa, M. *J. Phys. Chem.* **1994**, *98*, 2719−2721.
(27) Salama, T. M.; Shido, T.; Ohnishi, R.; Ichikawa, M. *J. Phys. Chem.* **1996**, *100*, 3688−3694.
(28) Gao, Z. X.; Sun, Q.; Chen, H. Y.; Wang, X.; Sachtler, W. M. H. *Catal. Lett.* **2001**, *72*, 1−5.
(29) Mohamed, M. M.; Salama, T. M.; Ohnishi, R.; Ichikawa, M. *Langmuir* **2001**, *17*, 5678−5684.

(30) Fierro-Gonzalez, J. C.; Gates, B. C. *J. Phys. Chem. B* **2004**, *108*, 16999−17002.
(31) Mohamed, M. M.; Salama, T. M.; Ichikawa, M. *J. Colloid Interface Sci.* **2000**, *224*, 366−371.
(32) Qiu, S.; Ohnishi, R.; Ichikawa, M. *J. Chem. Soc., Chem. Commun.* **1992**, 1425−1427.
(33) Schröder, D. *Angew. Chem., Int. Ed.* **2010**, *49*, 850−851.
(34) Van Koningsveld, H.; Van Bekkum, H.; Jansen, J. C. *Acta Crystallogr.* **1987**, *B43*, 127−132.
(35) Morris, R. E.; Weigel, S. J.; Henson, N. J.; Bull, L. M.; Janicke, M. T.; Chmelka, B. F.; Cheetham, A. K. *J. Am. Chem. Soc.* **1994**, *116*, 11849−11855.
(36) Kennedy, G. J.; Lawton, S. L.; Rubin, M. K. *J. Am. Chem. Soc.* **1994**, *116*, 11000−11003.
(37) Sklenak, S.; Dědeček, J.; Li, C.; Wichterlová, B.; Gábová, V.; Sierka, M.; Sauer, J. *Angew. Chem., Int. Ed.* **2007**, *46*, 7286−7289.
(38) Olson, D. H.; Khosrovani, N.; Peters, A. W.; Toby, B. H. *J. Phys. Chem. B* **2000**, *104*, 4844−4848.
(39) Han, O. H.; Kim, C. S.; Hong, S. B. *Angew. Chem., Int. Ed.* **2002**, *41*, 469−472.
(40) Mentzen, B. F.; Sacerdote-peronnet, M. *Mater. Res. Bull.* **1994**, *29*, 1341−1348.
(41) Barone, G.; Casella, G.; Giuffrida, S.; Duca, D. *J. Phys. Chem. C* **2007**, *111*, 13033−13043.
(42) Lonsinger, S. R.; Chakraborty, A. K.; Theodorou, D. N.; Bell, A. T. *Catal. Lett.* **1991**, *11*, 209−217.
(43) Hansen, N.; Kerber, T.; Sauer, J.; Bell, A. T.; Keil, F. J. *J. Am. Chem. Soc.* **2010**, *132*, 11525−11538.
(44) Hansen, N.; Brüggemann, T.; Bell, A. T.; Keil, F. J. *J. Phys. Chem. C* **2008**, *112*, 15402−15411.
(45) Drake, I. J.; Zhang, Y.; Gilles, M. K.; Teris Liu, C. N.; Nachimuthu, P.; Perera, R. C. C.; Wakita, H.; Bell, A. T. *J. Phys. Chem. B* **2006**, *110*, 11665−11676.
(46) Zhang, Y.; Drake, I. J.; Briggs, D. N.; Bell, A. T. *J. Catal.* **2006**, *244*, 219−229.
(47) Nieminen, V.; Sierka, M.; Murzin, D. Y.; Sauer, J. *J. Catal.* **2005**, *231*, 393−404.
(48) Zhou, D.; Bao, Y.; Yang, M.; He, N.; Yang, G. *J. Mol. Catal. A: Chem.* **2006**, *244*, 11−19.
(49) Boekfa, B.; Choomwattana, S.; Khongpracha, P.; Limtrakul, J. *Langmuir* **2009**, *25*, 12990−12999.
(50) Maihom, T.; Pantu, P.; Tachakritikul, C.; Probst, M.; Limtrakul, J. *J. Phys. Chem. C* **2010**, *114*, 7850−7856.
(51) Wannakao, S.; Boekfa, B.; Khongpracha, P.; Probst, M.; Limtrakul, J. *ChemPhysChem* **2010**, *11*, 3432−3438.
(52) Wannakao, S.; Khongpracha, P.; Limtrakul, J. *J. Phys. Chem. A* **2011**, *115*, 12486−12492.
(53) Zhao, Y.; Truhlar, D. G. *J. Chem. Phys.* **2006**, 125.
(54) Zhao, Y.; Truhlar, D. G. *Acc. Chem. Res.* **2008**, *41*, 157−167.
(55) Zhao, Y.; Truhlar, D. G. *Theor. Chem. Acc.* **2008**, *120*, 215−241.
(56) Ferrighi, L.; Hammer, B.; Madsen, G. K. H. *J. Am. Chem. Soc.* **2009**, *131*, 10605−10609.
(57) Valero, R.; Gomes, J. R. B.; Truhlar, D. G.; Illas, F. *J. Chem. Phys.* **2008**, 129.
(58) Valero, R.; Gomes, J. R. B.; Truhlar, D. G.; Illas, F. *J. Chem. Phys.* **2010**, 132.
(59) Zhao, Y.; Truhlar, D. G. *J. Phys. Chem. C* **2008**, *112*, 6860−6868.
(60) Kumsapaya, C.; Bobuatong, K.; Khongpracha, P.; Tantirungrotechai, Y.; Limtrakul, J. *J. Phys. Chem. C* **2009**, *113*, 16128−16137.
(61) Madsen, G. K. H.; Ferrighi, L.; Hammer, B. *J. Phys. Chem. Lett.* **2009**, *1*, 515−519.
(62) Igel-Mann, G.; Dolg, M.; Wedig, U.; Preuss, H.; Stoll, H. *J. Chem. Phys.* **1987**, *86*, 6348−6351.
(63) Reed, A. E.; Curtiss, L. A.; Weinhold, F. *Chem. Rev.* **1988**, *88*, 899−926.
(64) Reed, A. E.; Weinhold, F. *J. Chem. Phys.* **1983**, *78*, 4066−4073.
(65) Frisch, M. J.; Trucks, G. W.; Schlegel, H. B.; Scuseria, G. E.; Robb, M. A.; Cheeseman, J. R.; Montgomery, J. A., Jr.; Vreven, T.; Kudin, K. N.; Burant, J. C.; Millam, J. M.; Iyengar, S. S.; Tomasi, J.; Barone, V.; Mennucci, B.; Cossi, M.; Scalmani, G.; Rega, N.; Petersson, G. A.; Nakatsuji, H.; Hada, M.; Ehara, M.; Toyota, K.; Fukuda, R.; Hasegawa, J.; Ishida, M.; Nakajima, T.; Honda, Y.; Kitao, O.; Nakai, H.; Klene, M.; Li, X.; Knox, J. E.; Hratchian, H. P.; Cross, J. B.; Adamo, C.; Jaramillo, J.; Gomperts, R.; Stratmann, R. E.; Yazyev, O.; Austin, A. J.; Cammi, R.; Pomelli, C.; Ochterski, J. W.; Ayala, P. Y.; Morokuma, K.; Voth, G. A.; Salvador, P.; Dannenberg, J. J.; Zakrzewski, V. G.; Dapprich, S.; Daniels, A. D.; Strain, M. C.; Farkas, O.; Malick, D. K.; Rabuck, A. D.; Raghavachari, K.; Foresman, J. B.; Ortiz, J. V.; Cui, Q.; Baboul, A. G.; Clifford, S.; Cioslowski, J.; Stefanov, B. B.; Liu, G.; Liashenko, A.; Piskorz, P.; Komaromi, I.; Martin, R. L.; Fox, D. J.; Keith, T.; Laham, M. A.; Peng, C. Y.; Nanayakkara, A.; Challacombe, M.; Gill, P. M. W.; Johnson, B.; Chen, W.; Wong, M. W.; Gonzalez, C.; Pople, J. A. *Gaussian 03*, revision B.05; Gaussian, Inc.: Pittsburgh, PA, 2003.
(66) Bishea, G. A.; Morse, M. D. *J. Chem. Phys.* **1991**, *95*, 5646−5659.
(67) Schwerdtfeger, P.; Lein, M.; Krawczyk, R. P.; Jacob, C. R. *J. Chem. Phys.* **2008**, 128.
(68) Roldan, A.; Ricart, J. M.; Illas, F.; Pacchioni, G. *Phys. Chem. Chem. Phys.* **2010**, *12*, 10723−10729.
(69) Roldán, A.; González, S.; Ricart, J. M.; Illas, F. *ChemPhysChem* **2009**, *10*, 348−351.
(70) Boekfa, B.; Pantu, P.; Probst, M.; Limtrakul, J. *J. Phys. Chem. C* **2010**, *114*, 15061−15067.